Optimization of Distributed Integrated Multi-energy System Considering Industrial Process Based on Energy Hub

Yizhi Zhang, *Student Member*, *IEEE*, Xiaojun Wang, *Member*, *IEEE*, Jinghan He, *Fellow*, *IEEE*, Yin Xu, *Senior Member*, *IEEE*, and Wei Pei, *Member*, *IEEE*

***Abstract*—As a typical scenario of distributed integrated multi-energy system (DIMS), industrial park contains complex production constraints and strong associations between industrial productions and energy demands. The industrial production process (IPP) consists of controllable subtasks and strict timing constraints. Taking IPP as a control variable of optimal scheduling, it is an available approach that models the IPP as material flow into an extension energy hub (EH) to achieve the optimization of industrial park. In this paper, considering the coupling between the production process and energy demands, a model of IPP is proposed by dividing the process into different adjustable steps, including continuous subtask, discrete subtask, and storage subtask. Then, a transport model of material flow is used to describe the IPP in an industrial park DIMS. Based on the concept of EH, a universal extension EH model is proposed considering the coupling among electricity, heat, cooling, and material. Furthermore, an optimal scheduling method for industrial park DIMS is proposed to improve the energy efficiency and operation economy. Finally, a case study of a typical battery factory is shown to illustrate the proposed method. The simulation results demonstrate that such a method reduces the operation cost and accurately reflects the operation state of the industrial factory.**

***Index Terms*—Distributed integrated multi-energy system (DIMS), industrial production process (IPP), energy hub (EH), optimal operation, battery production.**

I. Introduction

DISTRIBUTED integrated multi-energy system (DIMS) integrates the generation, transmission, consumption, and storage of multiple energy systems, including electricity, heat, cooling, and gas together [1], [2], which is an effective technology to achieve higher efficiency and reliability [3]. Because of the relatively steady energy demand with higher energy density, industrial park is a typical DIMS and has been widely deployed in practice. Meanwhile, compared with residential and commercial consumers, industrial facilities consume more energy, with about 54% of the total delivered energy of the world [4]. Besides, the most critical energy demand in industrial parks is the production load. It is an important project to improve the energy utilization efficiency of industrial production to promote the energy development.

For industrial park DIMS, industrial production process (IPP) provides additional flexibility and coupling. Compared with general DIMS, managers of industrial park can control the operation status from both sides of supply and demand. On the supply side, similar to general DIMS, there are many types of local energy devices such as combined heat and power (CHP), photovoltaic (PV) power, as well as other energy conversion devices such as heat pump (HP), absorption chiller (AC), etc. [5], [6]. On the demand side, industrial parks operate with complex production processes corresponding to multiple energy demands, which is conventionally considered as a polymerized load. However, IPP is a combination of various steps and can be divided into multiple adjustable subtasks. IPP provides more control means and flexibility to match the adjustment of energy system. The coupling between IPP and energy demands can contribute to the optimization of the whole energy system in industrial factory, which reduces the manufacturing costs. In this way, industrial park DIMS can be scheduled by integrating IPP and DIMS.

There have been numerous theoretical studies for the operation optimization of DIMS in the modeling method and system analysis [7]-[15]. In 2007, the Swiss Federal Institute of Technology put forward the concept of energy hub (EH) [10], which is a universal DIMS model to describe the conversion and distribution of multiple energies. The EH-based model facilitates the calculation of energy flows in DIMS, as well as the optimization of operation and planning [11]. To improve the applicability of EH, numerous improved EH modeling methods have been proposed. Since then, the concept of the coupling matrix in EH is widely applied for the studies of industrial parks [12], residential consumers [13], and commercial buildings [14]. Among them, [15] has made further studies on the standard matrix modeling method of

Manuscript received: April 26, 2020; accepted: August 5, 2020. Date of CrossCheck: August 5, 2020. Date of online publication: September 18, 2020.

This work was supported by the National Nature Science Foundation of China (No. 51977005).

Y. Zhang, X. Wang (corresponding author), J. He, and Y. Xu are with the School of Electrical Engineering, Beijing Jiaotong University, Beijing 100044, China (e-mail: 18117031@bjtu.edu.cn; xjwang1@bjtu.edu.cn; jjhe@bjtu.edu.cn; xuyin@bjtu.edu.cn).

W. Pei is with the Institute of Electrical Engineering, Chinese Academy of Sciences, Beijing 100190, China (e-mail: peiwei@mail.iee.ac.cn).

DOI: 10.35833/MPCE.2020.000260

EH. Research on steady-state energy flow calculation based on EH method has gradually matured.

While there are some research and engineering practices in the collaborative optimization of DIMS in industrial parks, very few papers follow the relationship between DIMS and IPP. For industrial DIMS, most studies mainly focus on the optimal scheduling of energy systems. References [16]-[18] propose an operation strategy to reduce the operation costs considering multiple energy supply and energy storage (ES), but the constraints of industrial production are generally considered as fixed load. On the other hand, considering the flexibility of industrial loads, the optimization methods of DIMS based on demand response have been presented in recent years [19]-[21]. But these methods treat industrial loads as load aggregates that cannot describe the constraints of production process, which causes difficulties in managing specific devices in practice. Since then, the optimal scheduling method considering IPP is needed for industrial park DIMS. Furthermore, current research on IPP mainly focuses on power systems. Reference [22] proposes a management scheme for industrial parks based on the state task network (STN), and a method to model IPP as a mathematical model including discrete and continuous variables. References [23], [24] further propose optimal energy management considering on-site generation. However, current research mainly optimizes production by responding to electricity pricing and ignores the coupling of DIMS and IPP. Reference [25] preliminarily verifies the feasibility of joint optimization of the production process and energy systems. However, the analysis of IPP in the paper focuses on the production constraints and lacks the research on the coupling between IPP and DIMS. Overall, for the optimization of IPP and DIMS, there is currently a lack of universal unified modeling and optimization method considering the constraints of IPP in industrial parks.

For industrial park DIMS, actually, the present scheduling strategy is a two-stage method. Firstly, IPP is managed based on electricity pricing to obtain energy demand. Then, the energy system is optimized to meet the demand. A universal unified model combining DIMS and IPP is also needed for the optimization of industrial park. This paper addresses this issue by establishing a universal extension EH model considering IPP as material flow. The coordinative optimization of DIMS and IPP can achieve economical operation for industrial park DIMS. This paper makes the following contributions:

1) It proposes a universal model for IPP dividing the whole process into three types of subtasks according to the operation characteristics and describing the coupling with energy system.

2) IPP is modeled as material flow, and a standard modeling method for industrial parks is proposed combining IPP and DIMS. The universal extension EH model considering IPP is established to analyze the generalized energy flow for industrial park DIMS.

3) Based on the extension EH for industrial park DIMS, an optimal scheduling strategy is proposed to reduce operation costs by adjusting industrial production and energy supply. A battery factory is presented to test the proposed method.

The rest of this paper is organized as follows. Section II explains a universal model for IPP. Section III establishes the unified extension EH model considering the material flow of IPP. Section IV describes a typical IPP of a battery factory and develops the optimal scheduling model. A case study for a standard battery factory is presented to illustrate the proposed method in Section V. Finally, conclusions are summarized in Section VI.

II. Universal Model of IPP

The goal of industrial production is to accomplish planned yield, which follows the transfer of raw materials. A complete IPP is frequently a combination of a series of complex processes with strict timing constraints. The raw material is transformed on assembly lines, accompanied by multiple energy consumption, including cooling, heat, and electricity. Therefore, we first need to model IPP according to material flow based on the framework and constraints of actual production.

A. Framework of IPP

A complete IPP consists of different steps from material to semi-finished material, with the end to final products. There are a series of assembly lines in different workstations in complex production. Besides, different factories have different products and production processes. Since then, a universal framework is needed to describe IPP for industrial park DIMS.

From the standpoint of scheduling, IPP can be regarded as a series-parallel system that assumes material as a medium, different production devices as nodes, and transmission processes as branches. IPP can be described based on graph theory. We define the relatively continuous pipelines as an aggregate that can transform the input of raw materials to the output of semi-finished materials. The transfer process of material between different subtasks is defined as a line.

As IPP is accompanied by personnel deployment and numerous industrial devices, it is difficult for traditional device-level control method to directly manage IPP for the optimal scheduling of DIMS. To describe the actual IPP, these aggregative subtasks are further divided into different types according to their operation characteristics. Aiming at taking full advantage of the adjustability of IPP, it is necessary to consider the timing constraints between various links. If there are tight timing constraints between subtasks, it would be difficult for a single link to adjust independently within one scheduling period.

In the actual process, taking the packing link as an example, which is common in most factories, it usually includes several specific steps such as cutting, welding, forming, etc. These particular steps must operate in a specific order. The timing constraints among these steps are strict. For modern production, efficiency and standardization are important features. There is no obvious interval in these subtasks of packing link, which means that the manager cannot independently control the operation of each device. These specific devices should be integrated into aggregated subtasks according to reasonable standards to achieve adequate control.

When setting subtasks, the timing constraints among devices are important. Subtasks should contain a series of devices with strict timing constraints and can be scheduled independently. In an actual factory, there are storage links to store material. The warehouse is used to store semi-finished products and becomes a decoupling link in IPP. Based on storage links, IPP is defined with three subtasks, including continuous subtask, discrete subtask, and storage subtask.

1) Continuous Subtask

This type of subtask represents a set of continuous steps with strict timing constraints that cannot run independently before the previous step has been produced. In the interaction of energy system, continuous subtask can be compared to a device with fixed power, and what we can control is the working state that could be on or off. The typical case is the single-direction pipeline operation.

2) Discrete Subtask

This type of subtask represents a type of cumulative task, in which semi-finished materials should be processed in several consecutive periods. In this way, we can adjust the operation point without strict timing constraints by controlling the number of products. The discrete subtask can be regarded as a device we can manage with flexible and adjustable power besides switching state. The typical representation is the battery charge and discharge testing.

3) Storage Subtask

This type of subtask is used to describe the warehouse of materials. It is similar to energy storage in terms of operation characteristics. There are identical constraints among the input, output, and capacity compared with energy storage.

A framework of IPP is illustrated in Fig. 1, whose core part is the layout from the materials into the final product. The entire process can be decomposed into several subtasks due to the decoupling of the storage. This process can be regarded as a series structure where each subtask contains several separate production steps at the same time. Accompanying the whole production, there are also auxiliary devices such as lighting and lifting in the factory. Based on this framework, a complex production process can be simplified into a combination of several production subtasks and storage subtasks. Since the scheduling of production task is not only designed to start and stop devices, but also involves worker scheduling, it can effectively reduce the required control commands and have practical operability by characterizing a set of multiple devices with one subtask.

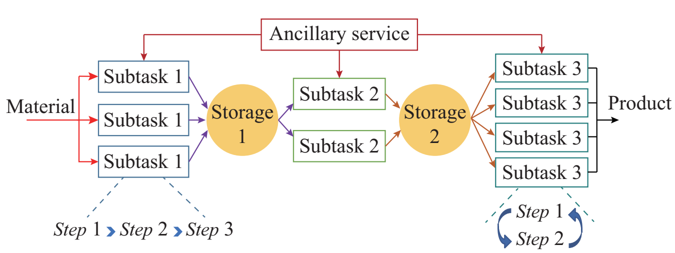

Fig. 1. Framework of IPP.

B. Constraints of IPP

The delivery of material is a physical link among different processes. The constraints of products determine the energy demand of industrial production because the output of production is directly related to energy consumption. Therefore, a mathematical model of production constraints is firstly established based on material production and transfer.

1) Continuous Subtask

The characteristic of continuous subtask is that only the on-off state of workstation can be controlled without constant adjustment. In addition, the minimum switching time constraint of each subtask is necessary. Formula (1) indicates the relationship between the state of subtask and start-stop variable. Since a subtask actually contains several lines with strict timing constraints and on-off time needs to show the constraints of the complete process, it is necessary to consider the constraints of the minimum running time and minimum downtime, as shown in (2). And (3) shows the output constraint of a subtask.

$$\begin{cases} v_{i,t}^{\alpha}-d_{i,t}^{\alpha}=u_{i,t}^{\alpha}-u_{i,t-1}^{\alpha} \\ v_{i,t}^{\alpha}+d_{i,t}^{\alpha}\leq 1 \end{cases} \tag{1}$$

$$\begin{cases} \sum\limits_{t=h}^{h+T_{i,off}^{\min}-1} u_{i,t}^{\alpha}\geq T_{i,on}^{\min} \\ \sum\limits_{t=h}^{h+T_{i,off}^{\min}-1} \left(1-u_{i,t}^{\alpha}\right)\geq T_{i,off}^{\min}u_{i,h}^{\alpha} \end{cases} \tag{2}$$

$$K_{t,sum}^{\alpha}=\sum_{i=1}^{N}u_{i,t}^{\alpha}K_{i}^{\alpha} \tag{3}$$

where α is a kind of continuous subtask; $u_{i,t}^{\alpha}$ is the switching status of the i^{th} workstation at time t; $v_{i,t}^{\alpha}$ and $d_{i,t}^{\alpha}$ are the switching actions of turning on and turning off, respectively; h is the h^{th} scheduling time; $T_{i,on}^{\min}$ and $T_{i,off}^{\min}$ are the minimum running and down time, respectively; K_{i}^{α} is the fixed output of each workstation; $K_{t,sum}^{\alpha}$ is the total output of the subtask at time t; and N is the number of workstations in the subtask.

2) Discrete Subtask

Compared with the continuous one, the output of discrete subtask is adjustable more than the switch state. Furthermore, the output of subtask can also be controlled. Compared with continuous subtask, the output K of discrete subtask is adjustable, and the output equation is shown in (4).

$$K_{t,sum}^{\beta}=\sum_{i=i}^{N_1}u_{i,t}^{\beta}K_{i,t}^{\beta} \tag{4}$$

where β is a kind of discrete subtask; $u_{i,t}^{\beta}$ is the switch status of the subtask; and $K_{i,t}^{\beta}$ is the adjustable output of the i^{th} workstation at time t.

3) Storage Subtask

The storage stage is a buffer between the two subtasks and decouples the two connected steps. Similar to energy storage, there are capacity constraints in the warehouse. Equation (5) shows the relationship between real-time capacity and input/output material, and (6) is the capacity limit.

$$S_{i,t}=S_{i,t-1}+\sum_{i=1}^{N_1}u_{i,t}^{in}K_{i,t}^{in}-\sum_{i=1}^{N_2}u_{i,t}^{out}K_{i,t}^{out} \tag{5}$$

$$S_{i,t}^{\min} \le S_{i,t} \le S_{i,t}^{\max} \tag{6}$$

where $S_{i,t}$ is the capacity of the storage stage at time t; $K_{i,t}^{in}$ and $K_{i,t}^{out}$ are the input and output yields of the storage, respectively; $u_{i,t}^{in}$ and $u_{i,t}^{out}$ are the switching status of the upstream subtask and downstream subtask, respectively; N_1 and N_2 are the numbers of workstations of upstream subtask and downstream subtask, respectively; and $[S_{i,t}^{\max}, S_{i,t}^{\min}]$ is the range of capacity.

C. Coupling of IPP and Energy System

The coupling of IPP and energy system is reflected in the energy demand of every subtask. To analyze the coupling relationship, IPP in an industrial park first needs to be divided into subtasks. For each subtask, the corresponding relationship between the energy demand and yield output of this subtask should be established. Through energy demand, IPP is connected with the energy system. To establish the coupling of IPP and energy system, the energy demand of IPP is further analyzed under the dispatching scale of the energy system.

Each subtask contains multiple production links. When calculating the power corresponding to a subtask, we need to select the rated power to represent the entire subtask collectively. Assuming that the subtask contains four production links, Fig. 2 shows the relationship between power and time. Each step in the figure represents the on/off of the corresponding devices. The red curve is the actual operation power of a subtask. The part enclosed by the red curve and the horizontal axis is the actual energy consumed. Due to the correspondence between closing sequence and opening sequence, the energy consumption during T_m, which means the stop time, can be equivalent to the area enclosed by the green curve and the red curve in the figure below. Therefore, the energy consumption of a production process can be equivalent to the rectangular area from the area of the stepped figure.

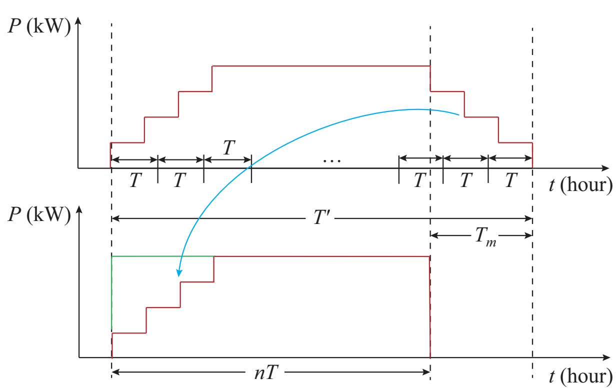

Fig. 2. Relationship between power and operation time.

In Fig. 2, T' is the actual running time; T_m is the time required for the device to turn on or off; T is the simulation period; and n is the number of simulations corresponding to the equivalent duration. Therefore, the equivalent power of the subtask is:

$$P = \frac{T'}{nT} P_e \tag{7}$$

where P is the rated power of the process at full operation; and P_e is the equivalent power of the process in scheduling.

In the scheduling, T' and T_m are known, and (7) is expressed as:

$$P = \frac{nT + T_m}{nT} P_e \tag{8}$$

The general model of IPP established in this paper includes three types of subtasks, the most special of which is the storage subtask. When it works, it stores and transfers semi-finished products, which does not involve processing. Therefore, it can be regarded as no interaction with the energy system except for general auxiliary loads such as conventional lighting and ventilation. For continuous subtasks and discrete sub-tasks, since there are clear production tasks and represent industrial machinery operation in modern factories, various loads that are closely related to the production volume will be generated. At the same time, in modern industrial production, in addition to electrical loads, there are often loads such as refrigeration, constant temperature and even steam, so the relationship between the subtask and the energy system is modeled as shown in (9):

$$\begin{cases} P_t^{\alpha} = \sum\limits_{i=i}^{N_1} u_{i,t}^{\alpha} K_i^{\alpha} P_i^{\alpha} \\ P_t^{\beta} = \sum\limits_{i=i}^{N_1} u_{i,t}^{\beta} K_{i,t}^{\beta} P_i^{\beta} \end{cases} \tag{9}$$

where P_t^{α} and P_t^{β} are the power of industrial load at time t; and $P_{i,t}^{\alpha}$ and $P_{i,t}^{\beta}$ are the load power of the i^{th} workstation at time t.

There is a significant difference between continuous subtask and discrete subtask. In continuous subtask, K_i^{α} is fixed and cannot be adjusted, but $K_{i,t}^{\beta}$ is an adjustable time-varying variable.

III. Extension EH Considering IPP

The mathematical model of IPP is given in the previous section. To achieve the collaborative optimization of IPP and DIMS, a universal model needs to be further established. EH is a typical method for analyzing the energy flow of DIMS, and the delivery of material can also be regarded as a kind of energy flow. Therefore, based on the concept of EH, an extension EH model considering material flow is established for industrial parks.

A. Concept of EH

An EH models a DIMS of any complexity as a unit with multiple input and output ports. The energy injected into the input ports, in the form of gas, electricity or other vectors, is described by a vector $\boldsymbol{V}_{in}$. Similarly, the outputs are described by a vector $\boldsymbol{V}_{out}$. The coupling matrix $\boldsymbol{C}$ defines the steady-state relationship between $\boldsymbol{V}_{in}$ and $\boldsymbol{V}_{out}$ at a specified period.

$$\boldsymbol{V}_{in} = \boldsymbol{C}\boldsymbol{V}_{out} \tag{10}$$

Figure 3 shows a simple DIMS which consists of a CHP unit and an AC. In this figure, the red, blue, yellow, and orange arrow represent the flow of heat, electricity, cooling, and fuel, respectively. The input of this DIMS shown as $v_{in,F}$ is gas. The outputs are electricity, heat, and cooling, which are shown as $v_{out,W}$, $v_{out,Q}$, and $v_{out,R}$. η_Q and η_W are the electricity and heat efficiency of CHP, respectively; η_R is the conversion efficiency of AC; and α_Q and α_R are the distribution coefficient of CHP power and heating generation, respectively.

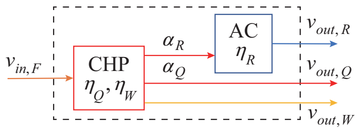

Fig. 3. Structure of EH.

This example is used here to illustrate how to establish an EH model. The input and output vectors of the EH model of this DIMS are:

$$V_{in} = \left[v_{in,F} \right] \tag{11}$$

$$V_{out} = \left[v_{out,R} \quad v_{out,Q} \quad v_{out,W} \right]^{\mathrm{T}} \tag{12}$$

The coupling matrix $\boldsymbol{C}$ is a 1×3 vector that can be written directly using energy dispatch and efficiency factors:

$$\boldsymbol{C} = \left[\eta_Q \alpha_R \eta_R \quad \eta_Q \alpha_Q \quad \eta_W \right] \tag{13}$$

When performing optimal scheduling calculations, the allocation coefficient is in matrix $\boldsymbol{C}$. Therefore, $\boldsymbol{C}$ is a time-varying matrix, and there are specific difficulties in solving the equations.

To facilitate the solving of the model, the distribution coefficient is converted into free energy flow through matrix transformation, and the EH model of the fixed coefficient matrix can be obtained. As described in [18], taking the structure of Fig. 3 as an example, the distribution coefficient α is expressed by the heat output energy flow of the CHP, and the input and output equations of EH are as follows:

$$V_{out} = \begin{bmatrix} 0 \\ \eta_Q \\ \eta_W \end{bmatrix} V_{in} + \begin{bmatrix} \eta_R \\ -1 \\ 0 \end{bmatrix} v_{QAC} \tag{14}$$

where v_{QAC} is the heat input to the AC produced by the CHP.

Compared with the traditional EH model based on the variable coefficient matrix, the EH model separately expresses the distribution coefficient in the form of branch energy flow. The coefficient matrix obtained by this method contains only the efficiency of device. The distribution coefficient participates in system scheduling with freedom degrees of energy flow. The following research is based on this model for further investigation.

B. Extension EH Considering Material Flow

In park-level systems, the EH model can adequately represent the flow direction and power. In the current EH model, loads are regarded as known conditions or aggregated loads that participate in the demand-side response. This method ignores a series of controllable conditions in industrial production.

When materials are transferred in different subtasks, although there is a morphological change, it can be regarded as a material flow in essence. This material flow includes nodes summarized by production subtasks and lines abstracted by the transmission process, which shows the same characteristics as the energy flow. Therefore, IPP is introduced into the EH model as material flow, and an extension EH model is established.

Through the modeling of IPP in Section II, the coupling of energy demand and yield output of subtask is established. It reflects the coupling of IPP and the energy system. The subtasks of IPP can be modeled as coupling devices that convert energy flow and material flow into material output. In this way, IPP is coupled with the energy system.

Compared with the energy system EH, the system input of the extension EH model adds raw materials, and the output adds the target products. The topology of the extension EH model is shown in Fig. 4, in which the purple arrow represents the flow of material. In Fig. 4, $v_{in,M}$ and $v_{out,M}$ are the input and output of material, respectively; η_{w1}, η_{m1}, η_{w2} and η_{m2} are the electricity and material conversion efficiencies of subtask 1 and subtask 2, respectively; and v_1-v_{11} are the energy flows from the initial node to the end node.

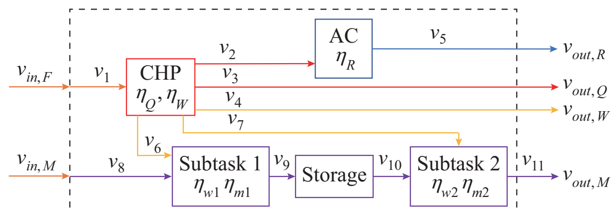

Fig. 4. Structure of extension EH.

According to the general IPP model established in section II, three types of subtasks are analyzed according to the EH model. In the EH model, devices are regarded as nodes. There are usually two types of nodes in EH, which are energy conversion node and energy storage node.

For continuous subtask and discrete subtask, they can be regarded as a node with multiple input ports and a single output port shown in Fig. 5. These two types of subtasks are similar to energy conversion elements, with energy and raw materials as input and semi-finished materials as output. Thus, the continuous and discrete subtasks can be modeled as a similar type of node as CHP and HP. In Fig. 5, v_{in} is the input of material; w_{in} is the input of energy; v_{out} is the output of semi-finished material; and η_w and η_m are the electricity and material conversion efficiencies of the subtask, respectively.

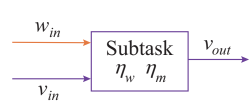

Fig. 5. Structure of subtask node.

For these subtasks, the node balance equation is given as:

$$\begin{cases} \boldsymbol{ZV} = \boldsymbol{0} \\ \begin{bmatrix} \dfrac{1}{\eta_{w1}} & \dfrac{1}{\eta_{m1}} & -1 \end{bmatrix} \begin{bmatrix} w_{in} \\ v_{in} \\ v_{out} \end{bmatrix} = 0 \end{cases} \tag{15}$$

where $\boldsymbol{Z}$ is the nodal energy conversion matrix of the subtask.

For the storage subtask, the model is relatively simple as there is no coupling of energy system. The storage subtask is regarded as a kind of energy storage system shown in Fig. 6, with similar form as battery energy storage system (BESS). v_{st} means the virtual branch that is connected to the "state of charge (SOC)".

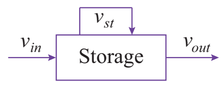

Fig. 6. Structure of storage subtask.

In order to maintain the unity of the format with other components, a virtual energy storage branch is added to the storage subtask. A'_g is used to present the original association matrix of storage. Considering the added branch, the node association matrix $\boldsymbol{A}_g$ of the storage component is:

$$\boldsymbol{A}_g = \begin{bmatrix} A'_g & 0 \\ 0 & -1 \end{bmatrix} \tag{16}$$

Further, the nodal energy conversion matrix is:

$$\boldsymbol{Z} = \begin{bmatrix} \eta_C & -\dfrac{1}{\eta_D} & -1 \end{bmatrix} \tag{17}$$

Based on the above analysis of the material flow, the complete extension EH model shown in Fig. 4. $\boldsymbol{Y}$, $\boldsymbol{Q}$, and $\boldsymbol{R}$ are the relevant parameter matrices. v_6, v_7, and v_8 are the items related to the material flow.

$$\boldsymbol{V}_{out} = \left[-\boldsymbol{Y}_1\boldsymbol{Q}_1^{-1}\boldsymbol{R} \right]\boldsymbol{V}_{in} + \left[\boldsymbol{Y}_2 - \boldsymbol{Y}_1\boldsymbol{Q}_1^{-1}\boldsymbol{Q}_2 \right]\boldsymbol{V}_2 = \begin{bmatrix} 0 & 0 \\ \eta_Q & 0 \\ \eta_W & 0 \\ 0 & \eta_{m1}\eta_{m2} \end{bmatrix} \begin{bmatrix} v_1 \\ v_8 \end{bmatrix} + \begin{bmatrix} 0 & 0 & 0 \\ -1 & 0 & 0 \\ 0 & -1 & -1 \\ 0 & \eta_{m2}\eta_{w1} & \eta_{w2} \end{bmatrix} \begin{bmatrix} v_2 \\ v_6 \\ v_7 \end{bmatrix} \tag{18}$$

The extension EH model above provides a method to describe the coupling between the energy system and IPP uniformly. Compared with the device of DIMS, the rated power of subtasks shown in (8) is not constant. For a given subtask, T_m is consistent, and the equivalent power is related to the duration of the subtask. Combined with the parameter settings in Fig. 5, the coefficient in (8) is equal to the energy utilization efficiency of the subtask. In this way, the subtask has the same expression form as the energy conversion device.

Equation (18) shows the complete energy flow constraint of DIMS and IPP at a time profile. For factories with different production processes, there are differences in the division of subtasks and the coupling between subtasks and energy system with varying demands of energy. However, the proposed method is a general modeling method. The structure of the coupling matrix is identical though different factories have different elements.

IV. Scheduling Model of Battery Factory

In this section, a battery factory is used as a case study to verify the proposed model. An extension EH model suitable for the battery factory is established through a detailed description of battery production. Besides, a collaborative scheduling model considering IPP is proposed.

A. Model of Battery Factory

According to the framework given in Section II, the process of battery production can be divided into three subtasks and two material storages (MS) of the semi-finished products. Firstly, the complete IPP of a battery factory is shown in Fig. 7. Raw material is sent to a subtask which is called "cell production (CP)". This subtask is used to produce battery cell. Then, cells can be stored and packed into the semi-finished battery through a packing line (PL), which is the second subtask. Finally, the semi-finished battery becomes the finished one through "formation and capacity grading (FG)", which means a repetition of charging and discharging.

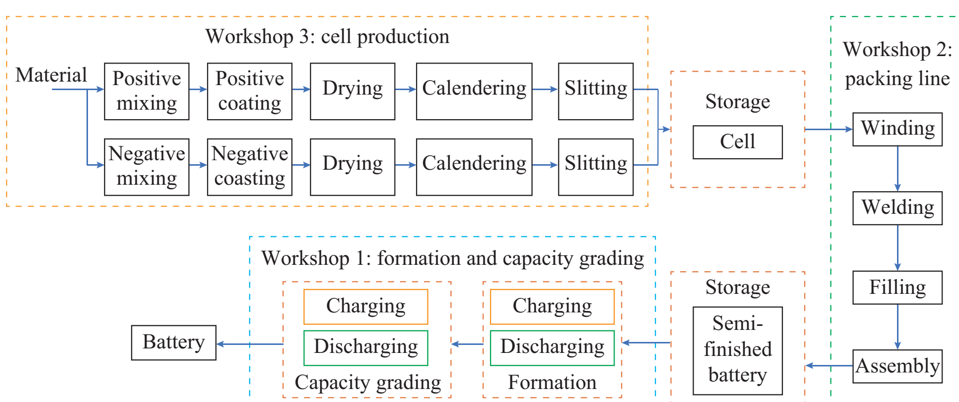

Fig. 7. Complete process of battery production.

In CP subtask, the raw material usually is processed through five links: mixing, coating, drying, calendering and slitting. There are strict timing constraints among these links, so the CP subtask is a continuous subtask. After CP, the raw material has been battery cell that can be stored in the first storage subtask and reprocessed in PL. Similar to CP, PL is also is a continuous subtask with four ongoing links: winding, welding, filling, and assembly. After this step, the semi-finished battery is produced and can be stored in the second storage subtask. In the last step, the semi-finished battery will be formatted and graded in FG. The number of batteries charging and discharging can be flexibly adjusted, which means FG is a discrete subtask. There is a unique characteristic in this subtask that the energy released during battery discharge can be fed back to the grid through the conversion cabinet.

From the perspective of material flow, the raw material becomes battery products after three subtasks. There are many industrial devices in CP, PL and FG, which are related to energy system. The energy demands for these three production subtasks are not only electricity, but also heat and cooling, which are used for specific different steps such as drying, constant temperature and cooling. The entire battery plant itself is a complete integrated energy system. Its functional equipment includes CCHP, PV, HP, AC, auxiliary boiler (AB), centrifugal chiller (CC), and energy storage systems, including BESS, thermal storage (TS), and cooling storage (CS).

In practice, there are more energy supply devices in the system where the number of freedom degrees has increased significantly. However, these freedom degrees are not entirely independent. For example, for subtask 1, the power source includes the grid purchase branch, PV branch, and CCHP power output branch. In the actual system regulation, the dispatcher will operate a combination of the three: the power flowing into subtask 1. Since the network constraints are not considered in the EH model, its connection relationship is an abstract concept, and there is no actual physical connection. With the introduction of virtual bus components, the system distribution coefficient will be uniformly reflected by the bus components, reducing the size of the matrix. The structure of the expanded EH model for the battery factory is shown in Fig. 8.

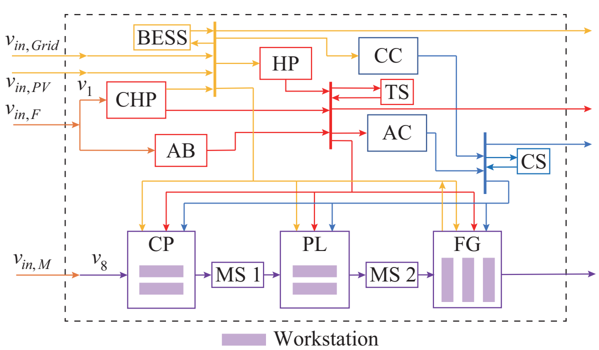

Fig. 8. Extension EH for battery factory.

B. Optimal Scheduling Model

The extension EH model introduced above primarily reflects the energy distribution under a single time profile. To optimize the operation of industrial park DIMS, an optimal scheduling model is needed based on the proposed extension EH model.

1) Objective Function

The goal of optimal scheduling is economic benefits. The daily production of the industrial park should follow the production plan. Under the same yield, the consumption of raw materials is fixed. The labor costs are billed monthly. The scheduling strategy would not cause changes in the consumption of raw materials and labor costs. Therefore, the objective function is defined as the minimization of DIMS operation cost.

Taking the above battery factory as an example for analysis, the operation cost of the energy system includes three parts: the cost of purchasing electricity, the cost of purchasing gas for the CHP unit, and the operation and maintenance costs of units. The operation and maintenance costs include start-up/shut-down costs of CHP and AC, maintenance costs of ES, and start-up/shut-down costs of IPP. The objective function of establishing the optimal scheduling model of the battery production factory is as shown in (19).

$$\begin{cases} F_1 = \min\left(C_{grid} + C_{gas} + C_{ope}\right) \\ C_{ope} = C_{CHP,start} v_{CHP,t} + C_{AC,start} v_{AC,t} + \sum C_{ES} P_{ES,i,t} + \\ \qquad \sum C_{start,IPP} v_{IPP,i,t} \end{cases} \tag{19}$$

where C_{grid} is the cost of purchasing electricity; C_{gas} is the cost of purchasing gas for the CHP unit; C_{ope} is the operation and maintenance costs of the devices; C_{start} is the start-up/shut-down costs of units; and C_{ES} is the maintenance cost of ES.

2) Constraints

First, there are constraints for the balance of extension EH.

The main constraints of system optimization are the energy balance constraints of DIMS and the material balance constraints of IPP.

This part of the constraint is reflected by the established extension EH model, which satisfies the EH equilibrium equation shown in (20).

$$\boldsymbol{V}_{out} = \left(-\boldsymbol{Y}_1 \boldsymbol{Q}_1^{-1} \boldsymbol{R}\right) \boldsymbol{V}_{in} + \left(\boldsymbol{Y}_2 - \boldsymbol{Y}_1 \boldsymbol{Q}_1^{-1} \boldsymbol{Q}_2\right) \boldsymbol{U} \boldsymbol{V}_2 \tag{20}$$

Second, there are constraints for the storage system.

Compared with energy conversion devices, the storage system is with visible timing characteristics. The stored energy is coupled at the next moments. Therefore, it is necessary to set the constraints of SOC. The storage devices in the extension EH include BESS, TS, CS and two storage subtasks.

Formula (21) is the operation constraints for ES, including timing constraint of SOC, range constraint of charging/discharging power, and range constraint of SOC.

$$\begin{cases} E_{ES,t} = E_{ES,t-1} + \Delta E_{ES,t} \\ \Delta E_{ES}^{\min} \le \Delta E_{ES,t} \le \Delta E_{ES}^{\max} \\ E_{ES}^{\min} \le E_{ES,t} \le E_{ES}^{\max} \\ \Delta E_{ES,t} = \eta_{ES} v_{ES,t} \end{cases} \tag{21}$$

where $E_{ES,t}$ is the rate of changes of the SOC at time t; $\Delta E_{ES,t}$ is the charging/discharging power; the supersripts min and max represent the minimum and maximum values of the variables, respectively; η_{ES} is the charging/discharging efficiencies; and $v_{ES,t}$ is the charging/discharging power of ES.

Third, there are also the constraints for conversion devices.

Formula (22) uniformly shows the constraints of energy conversion device, which separately indicates the rate of change of energy conversion and the range of output.

$$\begin{cases} E_{\alpha,t}^{out} = \lambda E_{\alpha,t}^{in} \\ E_{\alpha,t}^{out,\min} \le E_{\alpha,t}^{out} \le E_{\alpha,t}^{out,\max} \end{cases} \tag{22}$$

where $E_{\alpha,t}^{out}$ is the output power of device; $E_{\alpha,t}^{in}$ is the input power of device; and λ is the efficiency of energy conversion.

The energy flows in the extension EH should satisfy the comprehensive of energy flow equations as shown in (20)-(22). The constraints for IPP can refer to (1) and (2).

Finally, the proposed optimal scheduling model can be summarized as follows:

$$\begin{cases} \text{Objective function: (19)} \\ \text{s.t. (1), (2), (20)} - \text{(22)} \end{cases} \tag{23}$$

In this way, the complete optimal dispatch model of off-grid DIMS is obtained considering complex industrial processes. Since there is a product of the start-stop variable and the power variable in (2), this model is a nonlinear problem. To facilitate the calculation, this paper adopts the Big M method to linearize (2) [26].

In this way, the optimal model becomes a mixed-integer linear programming problem and can be solved by CPLEX, which is a mature commercial solver.

V. Case Study

A. Case Introduction and Verification

The extension EH model of the battery factory is established in the previous section. In this section, an actual battery factory, which is located in Guangdong, China, is used as a case to test the proposed method.

There are two workstations in CP, two workstations in PL, and four workstations in FG. The parameters of subtasks are shown in Table I. Especially, the loads of FG_d and FG_c are rated power. They can be adjusted continuously because of the manageable workload of FG.

TABLE I
Parameters of Subtasks

Subtask	No.	Electric load (kW)	Heat load (kW)	Cooling load (kW)
CP	2	2000	760	1020
PL	2	1050	460	750
FG_d/FG_c	4	[−400, 750]	85	120
Auxiliary	3	[70, 200]	-	-

The parameters of energy converters in this park are shown in Table II. The first parameters of BESS, TS and CS mean SOC and the second mean rated power.

In this paper, we define unit yield as a standard output in one hour. Unit yield is used to evaluate the production capacity of the industrial factory.

As the three subtasks in IPP, especially the continuous subtasks, contain multiple uninterruptible steps, the simulation step should not be set too short to prevent the frequent start-stop of the production line. Simultaneously, considering the time lag between the production line arrangement and the production, it is suitable for day-ahead scheduling optimization with 0.5 h as simulation timing. The daily yield is set as 24 unit yields.

TABLE II
Parameters of Energy Converters

Converter	Capacity (kW)	Efficiency
CHP	2000 (electric), 2667 (thermal)	0.3/0.4
PV	500	-
HP	3000	3.5
CC	4000	4
AC	2000	0.7
BESS	1000/1000	0.95/0.95
TS	1000/300	0.9/0.9
CS	2000/2000	0.87/0.9

Figure 9 shows the optimization results of IPP. The four variables represent the half-hourly output of the three subtasks. Especially, FG includes two steps: charging and discharging. In Fig. 9, the red prism means the output of CP within half an hour, yellow for PL, green for FG_c, and blue for FG_d, respectively For each subtask, the maximum output for every period is a half unit output.

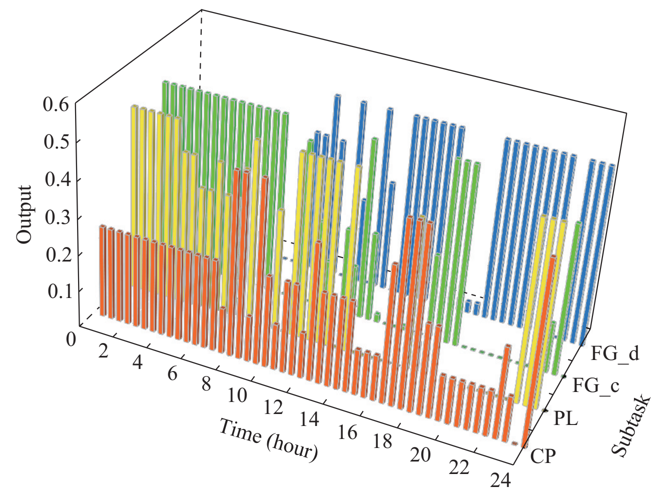

Fig. 9. Optimization results of IPP.

Figure 10 shows the changes in the inventory ratio of the cell storage and the semi-finished battery storage with 3 units of rated capacity.

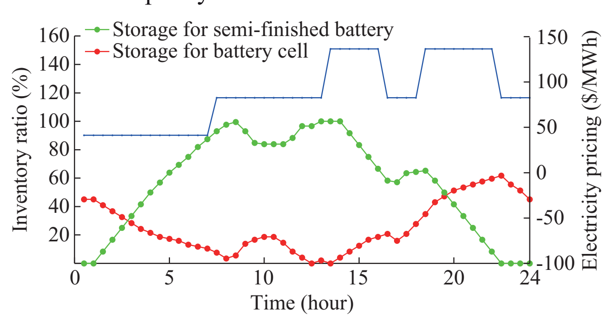

Fig. 10. Inventory ratio of two storage subtasks.

Based on the comprehensive analysis of Fig. 9 and Fig. 10, the output of PL is higher than that of CP in the first eight hours due to the initial storage capacity for battery cell. On the contrary, at the 8th hour, the capacity of storage for a semi-finished battery reaches the top. Overall, in the first eight hours, the outputs of CP, PL, and FG_c show high load operation. The most important reason is that the electricity pricing is lower during this period. For FG_d, the production is concentrated after 12 hours, as there is electricity released with production.

Figure 11 shows the simulation results of the energy supply and the load of IPP. Figure 11 (a), (b), and (c) are the optimization results of electricity, heat, and cooling systems, respectively, including the outputs of the various types of devices and the load requirements of IPP. The red line in Fig. 11 indicates the load corresponding to IPP. Corresponding to the load demand of three subtasks, electricity is the most critical load, which is mainly provided by power grid. For thermal and cooling systems, the main devices to supply energy are HP and CC because of their high conversion efficiency.

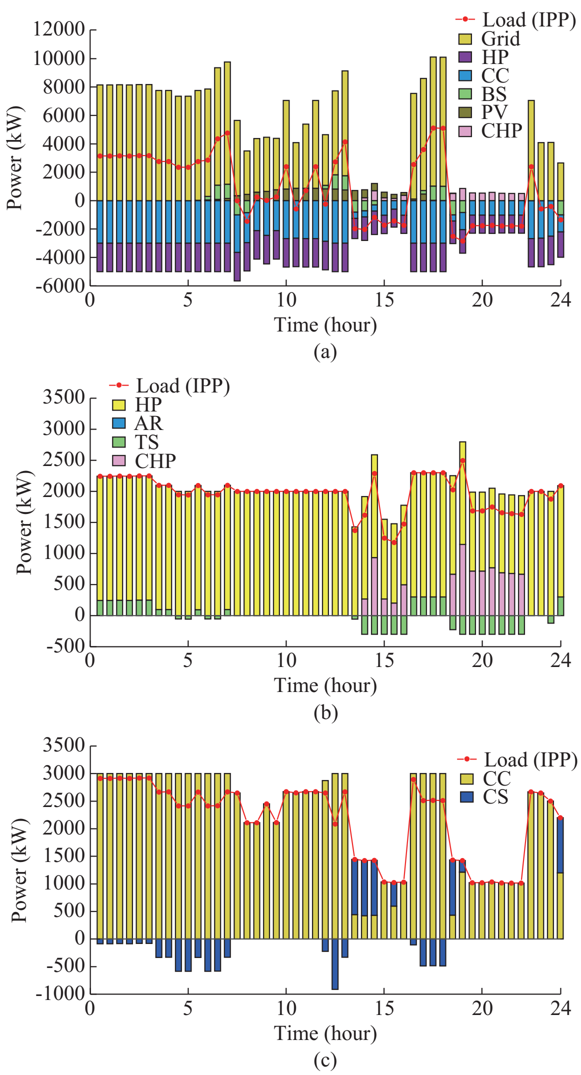

Fig. 11. Optimization results of DIMS. (a) Power system. (b) Thermal system. (c) Cooling system.

Combined with the electricity pricing in Fig. 10, it is found that the load of IPP in 1-7 h remains stable at about 3000 kW. During this period, the electricity pricing is the lowest. But as the limitation of semi-finished battery storage capacity, a part of the CP productions of are converted to 8-12 h and 16-18 h. In 13-16 h and 18-22 h with the highest electricity pricing, though the electric loads of IPP are negative, which is caused by the FG_d subtask, the heat loads and cooling loads are still more than 1000 kW, especially for the thermal system. The season of these results is the coupling of CHP and HP. CHP operates to reduce power purchased from power grid, which generates heat power. During these periods, CP subtasks keep working with the highest heat demand. The BESS in these two periods also discharges to support energy for HP that converts electricity to heat. The simulation results fully reflect the coupling between IPP and DIMS, and the coupling of electricity, heat and cooling system also affects the specific arrangement of the IPP process.

Besides the coupling of the electricity, heat and cooling system, the load transfer capability of ES effectively reduces the system operation costs. Table III shows the impact of BESS, TS and CS with different capacities. During simulation, only the capacity of one system can be changed, and the capacities of other two systems are set according to Table II. The overall trend is that as the capacity of the ES increases, the operation cost decreases. Since the heat load exhibits opposite to electricity and cooling load during the periods of high electricity prices, the changes in the capacity of TS have the most significant impact on the system operation costs.

TABLE III
IMPACT OF CAPACITY OF ES ON OPTIMIZATION

Storage	Capacity (kW)	Cost ($)
BESS	2000	7032
	1000	7136
	500	7190
	200	7222
TS	1500	7012
	1000	7136
	750	7209
	500	7249
CS	3000	7120
	2000	7136
	1500	7144
	1000	7152

B. Comparative Example Analysis

This section compares the superiority of the collaborative optimization method proposed in this paper with the existing optimization methods. The introduced battery factory is used as an example. In the current research, IPP is regarded as a regulation means to respond to electricity pricing. The IPP scheduling strategy is firstly obtained according to the electricity pricing, and then the DIMS is optimally scheduled to reduce the system operation costs. This two-stage method is compared with the unified modeling method proposed in this paper.

Case 1 is the optimization method based on the extension EH model and case 2 is optimized by a two-stage optimization method. The first stage optimizes IPP based on the time-of-use electricity pricing and obtains the cooling, heat, and electricity loads based on the known schedule of IPP. At the second stage, DIMS with certain loads is optimized based on EH model.

The DIMS unit outputs of the two methods with actual operation costs are further compared in Fig. 12. The results show that the total daily running cost of case 1 is lower than that of the two-stage calculation method. Due to lower electricity pricing, the cost of case 2 in the first seven hours is higher than that of case 1. Despite the low electricity pricing at this stage, due to the large concentration of IPP during this period, the heat and cooling loads increase, and the operation costs of CHP units increase.

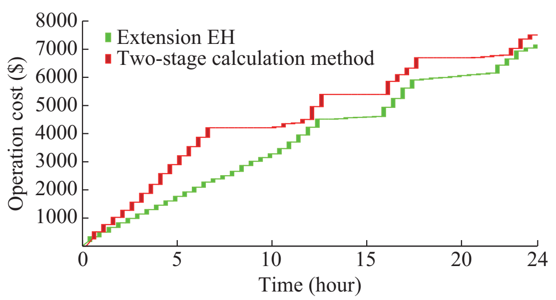

Fig. 12. Comparison of optimization costs for IPP.

In the context of industrial production with distinct integrated energy demands, the scheduling method of IPP in response to electricity pricing is unable to effectively utilize the coupling characteristics of DIMS. The collaborative optimization method of IPP and DIMS proposed in this paper can further reduce the production costs and improve the economic efficiency.

The coupling relationship between the DIMS system output and the IPP is established proving that the proposed extension EH model can perform collaborative optimization of DIMS and IPP.

The universal model proposed in this paper is based on the constraints of IPP. In addition to battery production factories, modern assembly line production companies such as steel smelting and chemical production also have similar constraints of IPP. For industrial parks with complex production processes and obvious energy demand, the modeling process of the extension EH model has applicability.

VI. Conclusion

IPP can be divided into different adjustable steps, including continuous and discrete subtasks and storage subtasks. IPP can be modeled as a material flow to establish a unified model with DIMS. The proposed extension EH model is a universal model, and it can describe the coupling relationship between IPP and DIMS. By linearizing the IPP model, this paper proposes a general optimized scheduling model for industrial parks. The general model established is a standard format, and it can be quickly built by IPP data card, which is suitable for various industrial parks. The simulation results show that coordinative optimization of DIMS and IPP can achieve economic system operation for industrial park DIMS.

Future works include the standard model considering system inertia for industrial park DIMS and the influence of social factors such as personnel arrangement. Besides, the problems caused by the probability of renewable energy and power failure are of further research interest.

References

[1] T. Krause, G. Andersson, K. Frohlich *et al.*, "Multiple-energy carriers: modeling of production, delivery, and consumption," *Proceedings of the IEEE*, vol. 99, no. 1, pp. 15-27, Jan. 2011.

[2] P. Sranislav, K. Bryan, and M. Tihomir, "Smart grids better with integrated energy system," in *Proceedings of 2009 IEEE Electrical Power & Energy Conference (EPEC)*, Montreal, Canada, Oct. 2009, pp. 1-8.

[3] M.C. Bozchalui, S. A. Hashmi, H. Hassen *et al.*, "Optimal Operation of residential energy hubs in smart grids," *IEEE Transactions on Smart Grid*, vol. 3, no. 4, pp. 1755-1766, Oct. 2012.

[4] X. Huang, S. Hong, and Y. Li, "Hour-ahead price based energy management scheme for industrial facilities," *IEEE Transactions on Industrial Informatics*, vol. 13, no. 6, pp. 2886-2898, Jun. 2017.

[5] G. Papaefthymiou, B. Hasche, and C. Nabe, "Potential of heat pumps for demand side management and wind power integration in the German electricity market," *IEEE Transactions on Sustainable Energy*, vol. 3, no. 4, pp. 636-642, Jul. 2012.

[6] H. Lund and E. Münster, "Integrated energy systems and local energy markets," *Energy Policy*, vol. 34, no. 10, pp. 1152-1160, Jul. 2006.

[7] Z. Li, W. Wu, J. Wang *et al.*, "Transmission-constrained unit commitment considering combined electricity and district heating networks," *IEEE Transactions on Sustainable Energy*, vol. 7, no. 2, pp. 480-492, Apr. 2016.

[8] Y. Wang, N. Zhang, C. Kang *et al.*, "Standardized matrix modeling of multiple energy systems," *IEEE Transactions on Smart Grid*, vol. 10, no. 1, pp. 257-270, Jan. 2019.

[9] X. Zhang, M. Shahidehpour, A. Alabdulwahab *et al.*, "Optimal expansion planning of energy hub with multiple energy infrastructures," *IEEE Transactions on Smart Grid*, vol. 6, no. 5, pp. 2302-2311, Jan. 2015.

[10] M. Geidl and G. Andersson, "Optimal power flow of multiple energy carriers," *IEEE Transactions on Power Systems*, vol. 22, no. 1, pp.145-155, Feb. 2007.

[11] Y. Wang, N. Zhang, and C. Kang, "Review and prospect of optimal planning and operation of energy hub in Energy Internet," *Proceedings of the CSEE*, vol. 35, no. 22, pp. 5669-5681, Nov. 2015.

[12] G. Chicco and P. Mancarella, "Matrix modelling of small-scale trigeneration systems and application to operational optimization," *Energy*, vol. 34, no. 3, pp. 261-273, Mar. 2009.

[13] T. Ha, Y. Zhang, V. V. Thang *et al.*, "Energy hub modeling to minimize residential energy costs considering solar energy and BESS," *Journal of Modern Power Systems and Clean Energy*, vol. 5, no. 3, pp. 389-399, May 2017.

[14] A. Piacentino, C. Barbaro, F. Cardona *et al.*, "A comprehensive tool for efficient design and operation of polygeneration-based energy μ grids serving a cluster of buildings, part I: description of the method," *Applied Energy*, vol. 111, pp. 1204-1221, Nov. 2013.

[15] Y. Wang, N, Zhang, C. Kang *et al.*, "Standardized matrix modeling of multiple energy systems," *IEEE Transactions on Smart Grid*, vol. 10, no. 1, pp. 257-270, Jan. 2019.

[16] J. Huan, M. Yu, H. Liu *et al.*, "Coordinated heat and power dispatch of industrial park microgrid considering distributed heating and indoor comfort constraint," in *Proceedings of 2017 IEEE Conference on Energy Internet and Energy System Integration (EI2)*, Beijing, China, Nov. 2017, pp. 2913-2918.

[17] F. Wang, H. Liu, Y. Chen *et al.*, "Optimal co-planning of park-level integrated heat and electricity energy systems," in *Proceedings of 2018 5th International Conference on Electric Power and Energy Conversion Systems (EPECS)*, Kitakyushu, Japan, Apr. 2018, pp. 7-12.

[18] W. Liu, J. Zhan, C. Y. Chung *et al.*, "Day-ahead optimal operation for multi-energy residential systems with renewables," *IEEE Transactions on Sustainable Energy*, vol. 10, no. 4, pp. 1927-1938, Oct. 2018.

[19] C. Dou, X. Zhou, T. Zhang *et al.*, "Economic optimization dispatching

strategy of microgrid for promoting photoelectric consumption considering cogeneration and demand response," *Journal of Modern Power Systems and Clean Energy*, vol. 8, no. 3, pp. 557-563, May 2020.

[20] T. Liu, D. Zhang, S. Wang *et al*., "Standardized modelling and economic optimization of multi-carrier energy systems considering energy storage and demand response," *Energy Conversion and Management*, vol. 182, pp. 126-142, Feb. 2019.

[21] Z. Jiang, Q. Ai, R. Hao *et al*., "Integrated demand response mechanism for industrial energy system based on multi-energy interaction," in *Proceedings of 2019 IEEE PES General Meeting*, Atlanta, USA, Aug. 2019, pp. 66336-66346.

[22] Y. Ding, S. Hong, and X. Li, "A demand response energy management scheme for industrial facilities in smart grid," *IEEE Transactions on Industrial Informatics*, vol. 10, no. 4, pp. 2257-2269, Jun. 2014.

[23] M. Choobineh and S. Mohagheghi, "Optimal energy management in an industrial plant using on-site generation and demand scheduling," *IEEE Transactions on Industry Applications*, vol. 52, no. 3, pp. 1945-1952, Dec. 2015.

[24] S. S. Reka and V. Ramesh, "Industrial demand side response modelling in smart grid using stochastic optimization considering refinery process," *Energy and Buildings*, vol. 127, pp. 84-94, Sept. 2016.

[25] X. Ma, W. Pei, H. Xiao *et al*., "Integrated energy network and production management optimization operation of battery production industrial estate considering complex production constraints," *Power System Technology*, vol. 42, no.11, pp. 3566-3575, Nov. 2018.

[26] Z. Zhou, P. Liu, Z. Li *et al.*, "An engineering approach to the optimal design of distributed energy systems in China," *Applied Thermal Engineering*, vol. 53, no. 2, pp. 387-396, May 2013.

Yizhi Zhang received the B.S. and M.Sc. degrees in electrical engineering from Beijing Jiaotong University, Beijing, China, in 2016 and 2018, respectively. He is currently pursuing the Ph.D. degree with Beijing Jiaotong University. His research interests include planning and operation of integrated energy system.

Xiaojun Wang received the B.S., M.Sc., and Ph.D. degrees in electrical engineering from North China Electric Power University, Beijing, China, in 2001, 2004, and 2008, respectively. In 2014, he was a Bond Scheme Scholar with ALTOM Grid, Stafford, U.K. He is currently an Associate Professor with Beijing Jiaotong University. His research interests mainly include planning and operation of integrated energy systems, the application of machine learning in power system operations, and fault location.

Jinghan He received the M.Sc. degree in electrical engineering from Tianjin University, Tianjin, China, in 1994, and the Ph.D. degree in electrical engineering from Beijing Jiaotong University, Beijing, China, in 2007. She is currently a Professor with Beijing Jiaotong University, Beijing, China. Her main research interests are protective relaying, fault distance measurement, and location in power systems.

Yin Xu received the B.E. and Ph.D. degrees in electrical engineering from Tsinghua University, Beijing, China, in 2008 and 2013, respectively. He is currently a Professor with Beijing Jiaotong University, Beijing, China. He is currently serving as Chair of Energy Internet Resilience Working Group under IEEE PES Energy Internet Coordinating Committee and Secretary of the Distribution Test Feeder Working Group under the IEEE PES Distribution System Analysis Subcommittee. His research interests include power system resilience, urban electricity-transportation integrated system, and power system high-performance simulation.

Wei Pei received the B.S. and M.S. degrees in electrical engineering from Tianjin University, Tianjin, China, in 2002 and 2005, respectively, and the Ph.D. degree from the Institute of Electrical Engineering, Chinese Academy of Sciences, Beijing, China, in 2008. He is currently working as a Professor with the Institute of Electrical Engineering, Chinese Academy of Sciences, Beijing, China, and with the University of Chinese Academy of Sciences, Beijing, China. He is also the Director of the Distributed Generation and Power System Research Group, Chinese Academy of Sciences. His research interests include integrated energy systems and AC/DC microgrid.